Electroencephalography and clinical Neurophysiology, 86 (1993) 7–14

EEG 92038

Determination of 10–20 system electrode locations using magnetic resonance image scanning with markers

Terrence D. Lagerlund [a], Frank W. Sharbrough [a], Clifford R. Jack, Jr. [b], Bradley J. Erickson [b], Dan C. Strelow [a], Kathleen M. Cicora [a] and Neil E. Busacker [a]

[a] *Department of Neurology and* [b] *Department of Diagnostic Radiology, Mayo Clinic and Mayo Foundation, Rochester, MN (USA)*

(Accepted for publication: 24 August 1992)

Summary We determined locations of 33 scalp electrodes used for electroencephalographic (EEG) recording by placing markers in the positions determined by the 10–20 system and performing magnetic resonance image (MRI) scanning on volunteer subjects. Small Vaseline-filled capsules glued on the scalp with collodion produced easily delineated regions of increased signal on standard MRI head images. Measurements of each capsule's coordinates in 3 dimensions were made from MRI scans. A spherical surface was fitted through the marker positions, giving an average radius and an origin (center of sphere). The coordinate axes were rotated to ensure that electrode C_z was on the z-axis and that the y-axis was oriented in the posterior-anterior direction. Two spherical (angular) coordinates were determined for each electrode. Spherical electrode coordinates for different subjects differed by less than 20° in all cases. An average and standard deviation of the spherical coordinates were calculated for each electrode. Standard deviations of several degrees were obtained. The average spherical coordinates obtained were close to those expected on the basis of applying the 10–20 system of placement to an ideal sphere. These measurements provide data necessary for various analyses of EEG performed to help localize epileptic foci.

Key words: Electrode coordinates; MRI scanning; Spherical coordinate system; Topographic maps; 10–20 System

Ascertainment of the distribution over the scalp surface of electrical potentials caused by cerebral generators is useful for identifying relevant activity patterns and components, for studying the topographic distribution of the activity patterns and components, and for proposing candidate generator structures and determining their locations. Localization of epileptic foci in patients being considered for surgical treatment for medically refractory epilepsy is one important clinical application. Mathematical techniques may be applied to scalp-recorded electroencephalographic (EEG) signals to enhance information about localization. Examples of this include construction of functional topographic maps through interpolation of scalp potentials to points between actual electrode positions (Perrin et al. 1987, 1989; Pascual-Marqui et al. 1988), source current density (Laplacian) estimation (Galambos et al. 1953; Hjorth 1975; Wallin and Stålberg 1980; Pascual-Marqui et al. 1988; Perrin et al. 1989), spatial deconvolution (estimation of cortical surface potentials from scalp potentials by using a model of volume conduction) (Nunez 1988), and source dipole localization (Salu et al. 1990). All these techniques require fairly precise knowledge about the locations, or coordinates, of all the scalp electrodes. We have measured these locations in normal subjects to assess the degree of variability in electrode positions between subjects and to provide electrode coordinates that can be used for analysis of EEG recordings.

Correspondence to: Dr. T.D. Lagerlund, Mayo Clinic, 200 First Street SW, Rochester, MN 55905 (USA).

Methods

Ten primary volunteer subjects (subjects 1–10, 7 females and 3 males) were studied. Each had 33 electrode positions marked by one of two EEG technicians using the 10–20 system, with a standard measurement technique agreed upon beforehand and verified by a physician electroencephalographer. The positions included 19 of the 21 standard 10–20 system electrode positions (omitting the ears) plus the nasion (N_z), inion (I_z), F_{pz}, and O_z positions, and the inferior temporal row of electrodes (F_9, FT_9, T_9, TP_{11}, P_9, F_{10}, FT_{10}, T_{10}, TP_{12}, and P_{10}; electrodes TP_{11} and TP_{12} are over the mastoid processes, and T_9 and T_{10} are at the preauricular points). Electrodes in these positions (Fig. 1) are routinely used for performing prolonged EEG recordings at the Mayo Clinic. Three additional volunteer subjects (subjects 11–13, all male) had 27 electrode positions marked (omitting FT_9, T_9, TP_{11}, FT_{10}, T_{10},

TABLE I

Measured angular coordinates (θ and ϕ), in degrees, of each electrode in 10 subjects.

		Subject									
		1	2	3	4	5	6	7	8	9	10
Radius (cm)		8.91	9.20	8.69	8.68	8.43	9.12	8.56	9.13	9.13	8.13
Midline electrodes											
N_z	θ	98.0	90.1	96.8	97.6	94.0	92.1	93.4	99.1	92.8	92.0
	ϕ	90.0	90.0	90.0	90.0	90.0	90.0	90.0	90.0	90.0	90.0
F_{pz}	θ	79.9	74.7	77.5	77.5	77.2	76.7	78.8	80.0	78.7	81.2
	ϕ	88.0	90.6	89.0	88.6	91.2	90.5	89.0	90.2	92.0	88.2
F_z	θ	41.3	39.7	40.7	42.6	39.7	39.5	42.5	41.7	39.4	42.6
	ϕ	85.1	88.2	91.5	89.1	90.1	91.7	90.0	87.7	93.1	90.4
C_z	θ	0.0	0.0	0.0	0.0	0.0	0.0	0.0	0.0	0.0	0.0
	ϕ	0.0	0.0	0.0	0.0	0.0	0.0	0.0	0.0	0.0	0.0
P_z	θ	44.3	43.4	40.1	44.5	41.0	42.2	44.4	45.9	43.8	45.1
	ϕ	271.0	268.3	267.5	268.3	268.8	272.5	268.7	271.9	269.5	269.6
O_z	θ	93.1	86.1	89.7	90.5	88.4	87.9	90.2	91.5	85.8	89.6
	ϕ	268.6	269.1	266.8	269.5	270.7	267.4	267.7	268.9	266.1	271.2
I_z	θ	113.0	110.5	112.4	111.0	105.0	107.3	109.2	109.5	102.7	111.5
	ϕ	266.5	270.8	267.0	267.7	269.6	266.0	268.2	267.9	265.8	268.0
10% parasagittal electrodes											
F_{p1}	θ	79.3	76.6	79.0	77.1	78.2	75.7	79.5	78.4	78.3	81.5
	ϕ	103.7	106.6	103.1	104.8	107.1	106.0	106.7	106.6	107.6	103.3
F_{p2}	θ	80.3	73.6	76.1	77.5	76.8	77.2	78.3	80.9	79.8	82.0
	ϕ	72.7	74.2	73.1	74.6	73.7	74.8	72.4	75.2	74.8	71.7
O_1	θ	89.7	88.2	90.9	88.1	88.8	87.7	90.3	90.6	–	88.9
	ϕ	253.8	253.7	250.4	251.5	247.5	246.9	249.4	252.0	–	250.7
O_2	θ	93.8	84.4	87.8	90.8	89.1	89.2	90.1	93.4	–	92.0
	ϕ	285.5	289.4	283.1	288.9	288.6	286.1	287.8	287.2	–	290.5
20% parasagittal electrodes											
F_3	θ	53.0	50.3	51.7	52.5	–	53.3	54.1	49.0	50.3	55.9
	ϕ	127.3	130.0	130.6	130.6	–	131.9	130.6	127.2	131.0	129.6
F_4	θ	55.3	51.3	50.4	51.5	54.2	50.9	54.3	54.8	57.5	56.1
	ϕ	47.2	51.4	47.8	50.1	50.8	50.9	48.7	51.4	46.9	53.1
C_3	θ	44.6	44.1	42.2	48.2	47.1	47.1	47.8	44.3	38.9	47.6
	ϕ	182.3	183.1	181.5	180.7	173.2	178.6	177.4	180.0	184.2	179.1
C_4	θ	46.5	43.4	43.8	46.3	41.8	46.0	49.5	46.5	50.2	46.3
	ϕ	−4.7	−3.2	−3.6	−4.3	0.0	2.0	−0.1	−1.6	3.1	2.7
P_3	θ	60.4	60.9	58.4	57.9	57.2	61.9	55.4	55.7	52.4	57.5
	ϕ	230.3	230.0	226.2	223.0	225.7	222.7	231.8	228.6	228.7	227.4
P_4	θ	62.6	52.6	56.5	59.9	57.5	60.1	61.6	60.1	53.8	57.4
	ϕ	308.2	308.8	304.9	309.6	314.8	318.2	317.1	312.9	315.4	314.6
40% parasagittal electrodes											
F_7	θ	84.2	80.6	84.2	84.4	80.4	84.7	85.2	84.6	76.2	86.7
	ϕ	135.3	138.7	132.9	138.0	138.7	136.5	136.7	135.8	143.2	135.8
F_8	θ	87.9	78.1	83.2	86.1	81.8	82.4	82.6	85.7	86.1	87.4
	ϕ	39.8	39.9	37.6	41.8	39.9	38.2	40.7	43.1	39.5	42.4
T_7	θ	94.3	97.2	96.1	97.1	95.0	97.6	98.5	94.1	84.4	95.5
	ϕ	174.3	176.8	169.8	173.6	172.3	176.8	173.6	175.0	176.7	170.6
T_8	θ	97.1	90.4	93.2	96.9	98.1	95.1	97.6	96.3	96.1	97.1
	ϕ	3.8	2.5	−0.2	2.2	1.2	7.2	−0.2	5.7	4.4	5.8
P_7	θ	95.0	91.7	93.6	96.3	90.6	103.3	88.7	90.0	88.9	91.3
	ϕ	216.8	217.9	215.8	215.1	212.6	214.2	216.2	217.9	221.6	213.3
P_8	θ	97.9	92.9	92.8	98.1	93.7	95.5	96.0	98.2	92.5	91.9
	ϕ	319.0	323.2	316.7	321.4	323.5	327.1	322.5	325.5	323.0	325.2
50% parasagittal electrodes											
F_9	θ	100.1	91.9	99.1	101.3	92.7	96.3	99.4	98.5	90.8	99.5
	ϕ	138.6	138.4	138.1	141.0	141.2	138.3	137.0	137.4	143.4	138.0
F_{10}	θ	102.2	93.0	98.2	103.0	95.4	92.7	98.8	98.9	98.4	100.3
	ϕ	40.2	43.0	34.8	40.5	38.0	41.1	42.2	41.9	33.4	41.6

TABLE I (continued)

		Subject									
		1	2	3	4	5	6	7	8	9	10
FT_9	θ	108.8	99.3	108.1	108.2	–	108.9	117.0	106.5	103.1	105.1
	ϕ	154.1	152.5	151.2	157.4	–	149.0	150.0	153.6	152.9	154.3
FT_{10}	θ	111.2	99.3	107.5	110.7	–	105.6	113.9	108.7	109.5	107.6
	ϕ	23.7	30.8	18.6	20.9	–	28.0	30.0	24.4	24.6	29.7
T_9	θ	115.8	116.7	121.5	122.1	117.8	117.6	123.2	114.7	113.1	118.1
	ϕ	172.0	162.5	166.5	174.3	167.8	161.6	160.1	166.0	168.2	167.3
T_{10}	θ	117.7	113.9	113.7	122.0	121.0	119.3	119.5	–	124.6	121.1
	ϕ	11.1	18.8	9.4	5.9	11.8	15.9	17.6	–	7.9	12.1
P_9	θ	111.6	107.6	115.4	112.5	110.0	119.9	107.9	108.0	104.7	107.5
	ϕ	219.0	216.6	215.1	218.7	209.6	209.9	214.1	218.7	216.2	213.5
P_{10}	θ	119.0	108.7	110.3	114.4	113.1	113.5	110.7	115.7	109.8	108.4
	ϕ	319.9	325.3	318.7	323.6	324.2	326.3	322.1	321.8	323.1	324.9
60% parasagittal electrodes											
TP_{11}	θ	127.7	132.7	131.5	134.3	129.2	131.1	128.6	123.9	127.1	125.1
	ϕ	197.7	189.0	194.7	203.7	198.5	191.9	197.9	197.9	199.3	202.1
TP_{12}	θ	130.9	126.3	125.9	135.2	129.8	131.1	123.7	131.8	133.5	126.4
	ϕ	341.1	349.0	342.8	338.3	337.0	347.1	340.7	342.0	330.2	335.8

and TP_{12}). In each of these 3 subjects, the electrode positions were marked by different EEG technicians, none of whom were involved with subjects 1–10. The technicians for subjects 11–13 also used the 10–20 system, but no attempt was made to standardize measurement techniques. (In fact, these 3 subjects were studied *before* the 10 primary subjects in a pilot study, and the experience with these 3 led to a decision for rigorously standardizing the measurement process for the primary subjects.) Small Vaseline-filled capsules were glued on the scalp in the marked electrode positions using collodion; these capsules produced easily delimited regions of increased signal on standard magnetic resonance imaging (MRI) scans of the head.

The MRI scans were displayed, and the center of each capsule was marked with a cursor. The x, y, and z coordinates of each marker were determined in the image coordinate system. A least-squares minimization

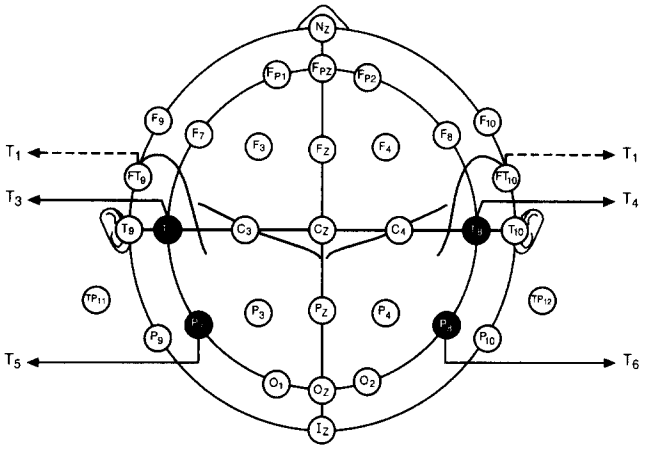

Fig. 1. Names and positions of the 33 electrodes used in the extended 10–20 system (modified combinatorial nomenclature).

algorithm determined the radius and center coordinates of a spherical surface that passed most nearly through the scalp marker positions. Electrode positions T_7 (same as T_3), T_8 (same as T_4), N_z, F_{pz}, F_{p1}, and F_{p2} were excluded from the fit because their distance from the center of the spherical surface differed from the radius of the sphere by more than 1.0 cm in most cases (T_7 in 8 of the 10 primary subjects, T_8 in 6 of the 10, and N_z, F_{pz}, F_{p1}, and F_{p2} in all primary subjects). In contrast, the electrode positions included in the fit had distances from the center of the spherical surface which differed from the radius of the sphere by more than 1.0 cm only occasionally (F_z in 5 of the 10 primary subjects and P_7 in 2 of the 10).

The electrode locations were converted by a rotation of the coordinate system to a standard system in which the z-axis passed through both the vertex (C_z) and the center of the best-fit spherical surface, and the nasion (N_z) was in the y-z plane. In this coordinate system, the x-axis ran from left to right, the y-axis from posterior to anterior, and the z-axis from inferior to superior. The rectangular (x, y, z) coordinates of each electrode location were converted to spherical coordinates (r, θ, ϕ) using the following formulas.

$$r = \sqrt{x^2 + y^2 + z^2}$$

$$\theta = \text{Arccos}\frac{z}{r}$$

$$\phi = \text{Arctan}\frac{y}{x}$$

Here, the value of the arctangent function (range, 0–360°) is chosen according to the signs of x and y (+/+, 0–90°; −/+, 90–180°; −/−, 180–270°; and +/−, 270–360°). The two angles ("latitude" and "longitude") represent the position of each electrode

TABLE II

The minimum, maximum, range, average, and standard deviation of the coordinates (θ and ϕ) for each electrode, in degrees.

		Subject (no.)	Minimum	Maximum	Range	Average	S.D.	Expected coordinates	Difference between average and expected
Midline electrodes									
N_z	θ	10	90.1	99.1	9.0	94.6	±3.0	112.5	−17.9
	ϕ		90.0	90.0	0.0	90.0	±0.0	90.0	0.0
F_{pz}	θ	10	74.7	81.2	6.5	78.2	±1.9	90.0	−11.8
	ϕ		88.0	92.0	4.0	89.7	±1.4	90.0	−0.3
F_z	θ	10	39.4	42.6	3.2	41.0	±1.3	45.0	−4.0
	ϕ		85.1	93.1	8.0	89.7	±2.3	90.0	−0.3
C_z	θ	10	0.0	0.0	0.0	0.0	±0.0	0.0	0.0
	ϕ		0.0	0.0	0.0	0.0	±0.0	0.0	0.0
P_z	θ	10	40.1	45.9	5.8	43.5	±1.9	45.0	−1.5
	ϕ		267.5	272.5	5.0	269.6	±1.7	270.0	−0.4
O_z	θ	10	85.8	93.1	7.3	89.3	±2.3	90.0	−0.7
	ϕ		266.1	271.2	5.1	268.6	±1.6	270.0	−1.4
I_z	θ	10	102.7	113.0	10.3	109.2	±3.3	112.5	−3.3
	ϕ		265.8	270.8	5.0	267.8	±1.6	270.0	−2.2
10% parasagittal electrodes									
F_{p1}	θ	10	75.7	81.5	5.8	78.4	±1.6	90.0	−11.6
	ϕ		103.1	107.6	4.5	105.5	±1.7	108.0	−2.5
F_{p2}	θ	10	73.6	82.0	8.4	78.2	±2.5	90.0	−11.8
	ϕ		71.7	75.2	3.5	73.7	±1.2	72.0	1.7
O_1	θ	9	87.7	90.9	3.2	89.2	±1.2	90.0	−0.8
	ϕ		246.9	253.8	6.9	250.6	±2.4	252.0	−1.4
O_2	θ	9	84.4	93.8	9.4	90.1	±2.9	90.0	0.1
	ϕ		283.1	290.5	7.4	287.5	±2.3	288.0	−0.5
20% parasagittal electrodes									
F_3	θ	9	49.0	55.9	6.9	52.2	±2.1	64.0	−11.8
	ϕ		127.2	131.9	4.7	129.9	±1.6	129.1	0.8
F_4	θ	10	50.4	57.5	7.1	53.6	±2.5	64.0	−10.4
	ϕ		46.9	53.1	6.2	49.8	±2.1	50.9	−1.1
C_3	θ	10	38.9	48.2	9.3	45.2	±3.0	45.0	0.2
	ϕ		173.2	184.2	11.0	180.0	±3.2	180.0	0.0
C_4	θ	10	41.8	50.2	8.4	46.0	±2.6	45.0	1.0
	ϕ		−4.7	3.1	7.8	−1.0	±2.9	0.0	−1.0
P_3	θ	10	52.4	61.9	9.5	57.8	±2.8	64.0	−6.2
	ϕ		222.7	231.8	9.1	227.4	±3.0	230.9	−3.5
P_4	θ	10	52.6	62.6	10.0	58.2	±3.3	64.0	−5.8
	ϕ		304.9	318.2	13.3	312.4	±4.4	309.1	3.3
40% parasagittal electrodes									
F_7	θ	10	76.2	86.7	10.5	83.1	±3.1	90.0	−6.9
	ϕ		132.9	143.2	10.3	137.2	±2.7	144.0	−6.8
F_8	θ	10	78.1	87.9	9.8	84.1	±3.0	90.0	−5.9
	ϕ		37.6	43.1	5.5	40.3	±1.7	36.0	4.3
T_7	θ	10	84.4	98.5	14.1	95.0	±4.0	90.0	5.0
	ϕ		169.8	176.8	7.0	173.9	±2.5	180.0	−6.1
T_8	θ	10	90.4	98.1	7.7	95.8	±2.4	90.0	5.8
	ϕ		−0.2	7.2	7.4	3.2	±2.6	0.0	3.2
P_7	θ	10	88.7	103.3	14.6	92.9	±4.4	90.0	2.9
	ϕ		212.6	221.6	9.0	216.1	±2.6	216.0	0.1
P_8	θ	10	91.9	98.2	6.3	94.9	±2.5	90.0	4.9
	ϕ		316.7	327.1	10.4	322.7	±3.1	324.0	−1.3
50% parasagittal electrodes									
F_9	θ	10	90.8	101.3	10.5	96.9	±3.8	103.7	−6.8
	ϕ		137.0	143.4	6.4	139.1	±2.0	149.4	−10.3
F_{10}	θ	10	92.7	102.9	10.2	98.1	±3.5	103.7	−5.6
	ϕ		33.4	43.0	9.6	39.7	±3.3	30.6	9.1
FT_9	θ	9	99.3	117.0	17.7	107.2	±4.8	108.7	−1.5
	ϕ		149.0	157.4	8.4	152.8	±2.5	164.3	−11.5

TABLE II (continued)

		Subject (no.)	Minimum	Maximum	Range	Average	S.D.	Expected coordinates	Difference between average and expected
FT_{10}	θ	9	99.3	113.9	14.6	108.2	±4.1	108.7	−0.5
	ϕ		18.6	30.8	12.2	25.6	±4.3	15.7	9.9
T_9	θ	10	113.1	123.2	10.1	118.0	±3.3	112.5	5.5
	ϕ		160.1	174.3	14.2	166.7	±4.4	180.0	−13.3
T_{10}	θ	9	113.7	124.6	10.9	119.2	±3.6	112.5	6.7
	ϕ		5.9	18.8	12.9	12.3	±4.4	0.0	12.3
P_9	θ	10	104.7	119.9	15.2	110.5	±4.5	103.7	6.8
	ϕ		209.6	219.0	9.4	215.1	±3.4	210.6	4.5
P_{10}	θ	10	108.4	119.0	10.6	112.4	±3.4	103.7	8.7
	ϕ		318.7	326.3	7.6	323.0	±2.4	329.4	−6.4
60% parasagittal electrodes									
TP_{11}	θ	10	123.9	134.3	10.4	129.1	±3.3	130.1	−1.0
	ϕ		189.0	203.7	14.7	197.3	±4.4	192.5	4.8
TP_{12}	θ	10	123.7	135.2	11.5	129.4	±3.7	130.1	−0.7
	ϕ		330.2	349.0	18.8	340.4	±5.5	347.5	−7.1

on the head surface and are independent of the subject's head size (although not entirely independent of head shape).

Finally, the minimum, maximum, mean, and standard deviation of the angles for subjects 1–10 were determined. The mean values were compared with those expected for the 10–20 electrode placements if the head were a sphere, with the vertex representing the "north pole" and with electrodes F_{pz}, T_7, T_8, and O_z being on the "equator."

Results

Table I shows the measured angular coordinates in degrees of each electrode for each of the 10 primary subjects. The best-fit sphere radius in centimeters is also given. Note that in subject 8, the capsule at site T_{10} was dislodged and not imaged; in subject 9, the capsules at sites O_1 and O_2 were not imaged; and in subject 5, the capsules at sites FT_9, FT_{10}, and F_3 were not imaged.

Table II shows the number of primary subjects studied and the minimum, maximum, range, average, and standard deviation of the angular coordinates in degrees for each electrode. The expected angular coordinates of each electrode are also shown, as is the difference between the expected value and the average of the measured values of the coordinates. Fig. 2 shows the average angular coordinates (θ, ϕ) for each electrode arranged according to the location of the electrode, and Fig. 3 shows the expected angular electrode coordinates.

Table III shows the average and standard deviation of the radii in centimeters and angular coordinates in degrees for each of 27 electrodes for subjects 1–10, the measured radius and angular coordinates for each electrode for subjects 11–13, and the differences between the measured values for subjects 11–13 and the average values for subjects 1–10. Note that in subject 12, the capsules at sites I_z, P_9, and P_{10} were dislodged and not imaged; and in subject 13, the capsules at sites F_9 and F_{10} were not imaged.

Discussion

The θ/ϕ coordinates for different subjects in the primary group (subjects 1–10) differed by less than

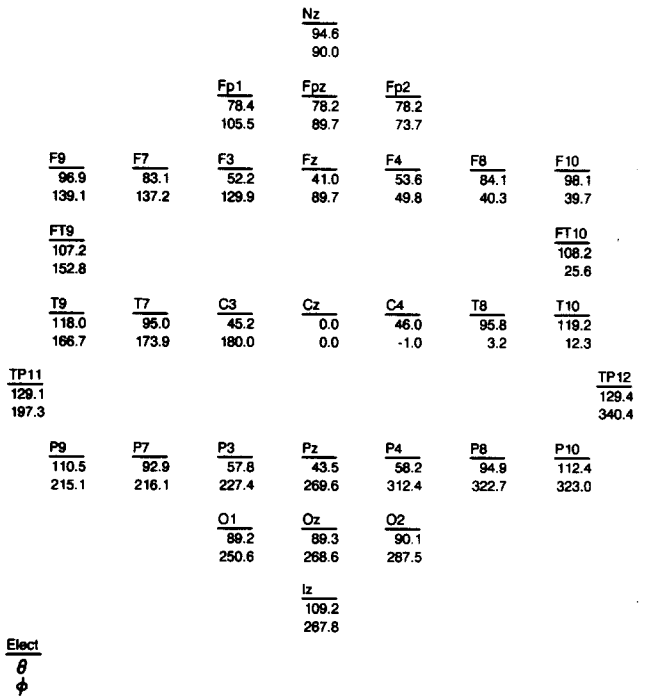

Fig. 2. Average measured angular (θ, ϕ) coordinates for each electrode (Elect).

TABLE III

Radius and angular coordinates (θ and ϕ): comparison of average values in 10 subjects with measured values in 3 additional subjects.

		Primary subjects 1–10		Subject 11		Subject 12		Subject 13	
		Average	S.D.	Measured value	Difference *	Measured value	Difference *	Measured value	Difference *
Radius (cm)		8.80	±0.36	8.83	−0.03	9.04	−0.24	9.20	−0.40
Midline electrodes									
N_z	θ	94.6	±3.0	94.9	−0.30	100.2	−5.60	90.6	4.00
	ϕ	90.0	±0.0	90.0	0.00	90.0	0.00	90.0	0.00
F_{pz}	θ	78.2	±1.9	75.7	2.50	80.1	−1.90	79.5	−1.30
	ϕ	89.7	±1.4	91.5	−1.80	88.3	1.40	90.9	−1.20
F_z	θ	41.0	±1.3	40.9	0.10	42.5	−1.50	46.1	−5.10
	ϕ	89.7	±2.3	87.9	1.80	88.6	1.10	87.4	2.30
C_z	θ	0.0	±0.0	0.0	0.00	0.0	0.00	0.0	0.00
	ϕ	0.0	±0.0	0.0	0.00	0.0	0.00	0.0	0.00
P_z	θ	43.5	±1.9	45.4	−1.90	40.7	2.80	51.4	−7.90
	ϕ	269.6	±1.7	268.6	1.00	267.8	1.80	267.6	2.00
O_z	θ	89.3	±2.3	97.6	−8.30	83.7	5.60	81.5	7.80
	ϕ	268.6	±1.6	270.8	−2.20	272.7	−4.10	272.3	−3.70
I_z	θ	109.2	±3.3	114.0	−4.80	–	–	92.3	16.90
	ϕ	267.8	±1.6	272.3	−4.50	–	–	272.0	−4.20
10% parasagittal electrodes									
F_{p1}	θ	78.4	±1.6	78.3	0.10	82.1	−3.70	80.2	−1.80
	ϕ	105.5	±1.7	105.3	0.20	104.6	0.90	107.6	−2.10
F_{p2}	θ	78.2	±2.5	79.0	−0.80	82.5	−4.30	80.9	−2.70
	ϕ	73.7	±1.2	76.0	−2.30	71.4	2.30	74.9	−1.20
O_1	θ	89.2	±1.2	98.8	−9.60	83.6	5.60	83.1	6.10
	ϕ	250.6	±2.4	252.9	−2.30	254.2	−3.60	258.0	−7.40
O_2	θ	90.1	±2.9	97.7	−7.60	84.6	5.50	80.4	9.70
	ϕ	287.5	±2.3	289.4	−1.90	290.5	−3.00	287.8	−0.30
20% parasagittal electrodes									
F_3	θ	52.2	±2.1	50.2	2.00	55.5	−3.30	55.7	−3.50
	ϕ	129.9	±1.6	130.8	−0.90	127.7	2.20	128.3	1.60
F_4	θ	53.6	±2.5	54.2	−0.60	55.6	−2.00	55.9	−2.30
	ϕ	49.8	±2.1	46.2	3.60	48.9	0.90	54.4	−4.60
C_3	θ	45.2	±3.0	42.6	2.60	48.0	−2.80	45.3	−0.10
	ϕ	180.0	±3.2	187.1	−7.10	178.8	1.20	178.3	1.70
C_4	θ	46.0	±2.6	45.9	0.10	46.2	−0.20	43.0	3.00
	ϕ	−1.0	±2.9	−3.7	−2.70	−0.1	−0.90	0.8	−1.80
P_3	θ	57.8	±2.8	61.2	−3.40	54.9	2.90	58.5	−0.70
	ϕ	227.4	±3.0	235.5	−8.10	224.4	3.00	231.8	−4.40
P_4	θ	58.2	±3.3	64.2	−6.00	55.0	3.20	53.1	5.10
	ϕ	312.4	±4.4	308.5	3.90	311.9	0.50	311.9	0.50
40% parasagittal electrodes									
F_7	θ	83.1	±3.1	82.7	0.40	87.4	−4.30	77.2	5.90
	ϕ	137.2	±2.7	137.9	−0.70	137.9	−0.70	142.2	−5.00
F_8	θ	84.1	±3.0	88.4	−4.30	88.2	−4.10	77.8	6.30
	ϕ	40.3	±1.7	46.0	−5.70	38.5	1.80	40.3	0.00
T_7	θ	95.0	±4.0	94.6	0.40	98.5	−3.50	79.0	16.00
	ϕ	173.9	±2.5	173.7	0.20	177.5	−3.60	181.1	−7.20
T_8	θ	95.8	±2.4	97.1	−1.30	95.3	0.50	80.5	15.30
	ϕ	3.2	±2.6	10.1	−6.90	1.9	1.30	4.0	−0.80
P_7	θ	92.9	±4.4	93.4	−0.50	91.9	1.00	81.0	11.90
	ϕ	216.1	±2.6	214.5	1.60	217.7	−1.60	222.4	−6.30
P_8	θ	94.9	±2.5	101.8	−6.90	92.0	2.90	78.3	16.60
	ϕ	322.7	±3.1	324.0	−1.30	322.6	0.10	324.1	−1.40
50% parasagittal electrodes									
F_9	θ	96.9	±3.8	100.6	−3.70	106.6	−9.70	–	–
	ϕ	139.1	±2.0	139.3	−0.20	139.3	−0.20	–	–
F_{10}	θ	98.1	±3.5	100.8	−2.70	106.8	−8.70	–	–
	ϕ	39.7	±3.3	45.6	−5.90	37.6	2.10	–	–

TABLE III (continued)

		Primary subjects 1–10		Subject 11		Subject 12		Subject 13	
		Average	S.D.	Measured value	Difference *	Measured value	Difference *	Measured value	Difference *
P_9	θ	110.5	±4.5	109.7	0.80	–	–	90.2	20.30
	ϕ	215.1	±3.4	210.7	4.40	–	–	220.2	−5.10
P_{10}	θ	112.4	±3.4	115.5	−3.10	–	–	86.1	26.30
	ϕ	323.0	±2.4	323.0	0.00	–	–	325.3	−2.30

* Difference between measured value of subject and average value of subjects 1–10.

17.7°/18.8° in all cases, and standard deviations were less than ±4.8°/5.5° (Table II), which demonstrated the reproducibility of electrode placement by one technician from subject to subject. However, differences between the θ/ϕ coordinates for subjects 11–13 differed from the average of subjects 1–10 by as much as 26.3°/8.1°, indicating that somewhat greater variability (at least in θ) was introduced when measurements were made by different technicians.

Also, the average θ/ϕ coordinates for subjects 1–10 were within 17.9°/13.3° of those expected on the basis of applying the 10–20 system of placement to a sphere. However, there were greater deviations from the expected values in electrodes N_z, F_{pz}, F_{p1}, F_{p2}, F_3, F_4, F_9, FT_9, T_9, and T_{10}. These electrodes are either in the frontal or temporal region where the head deviates significantly from a sphere (bulged frontally and depressed temporally). Although this geometric distortion seems to explain adequately the systematic deviations between the measured and ideal spherical coordinates, we cannot exclude the possibility of some additional bias introduced by the measurement technique used by the technician, even though this was closely supervised and standardized.

The average angular coordinates for subjects 1–10 are qualitatively similar to those obtained in a previous study (Law and Nunez 1991), in which electrode positions were determined using a commercial 3-dimensional digitizer and fitted to a sphere. Standard deviations were also similar in the two studies. In the previous one, the direction of the z-axis was determined by requiring that electrodes T_3, T_4, and O_z lie in the x-y plane, rather than requiring the z-axis to pass through C_z, and the direction of the x-axis was such as to pass nearly through the O_1 and F_{p2} electrodes rather than near T_7 and T_8. Consequently, the ϕ coordinates in the previous study differ from those given in Table II by about 258°. The θ coordinates of the frontal electrodes in the previous study (F_{p1} = 79.8, F_{p2} = 78.7, F_7 = 84.3, F_8 = 81.9) showed a trend to deviate from

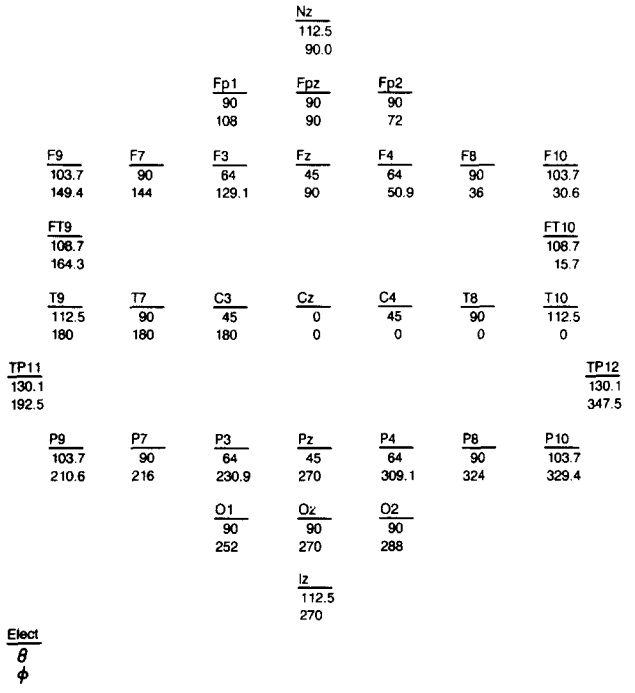

Fig. 3. Expected angular (θ, ϕ) coordinates for each electrode (Elect), assuming a spherical head and standard 10–20 system placement.

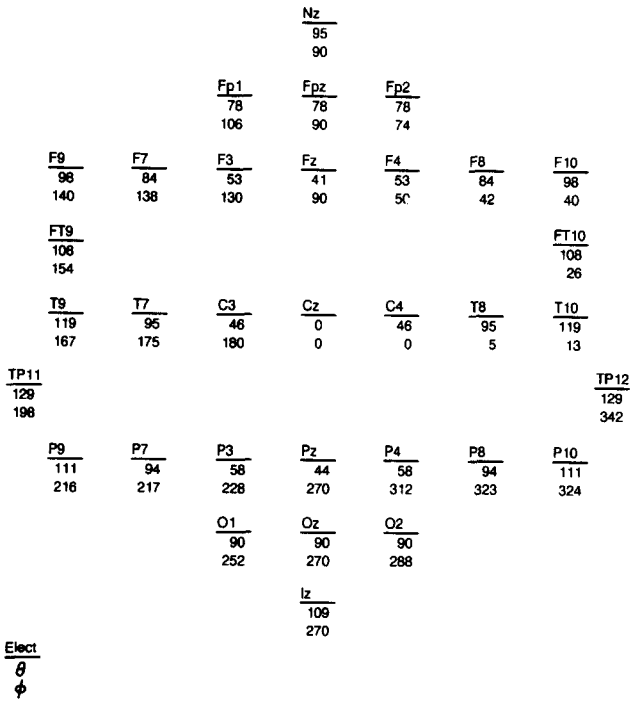

Fig. 4. Rounded angular (θ, ϕ) coordinates for each electrode, taking into account symmetry considerations.

the expected 90°, as was noted in our data ($F_{p1} = 78.4$, $F_{p2} = 78.2$, $F_7 = 83.1$, $F_8 = 84.1$); this finding suggests that bias due to the technician's measurement technique is not likely the major cause of these differences.

By symmetry considerations, it would be expected that θ coordinates of homologous electrodes over the left and right hemispheres would be identical. Similarly, the ϕ coordinate of each electrode on the right should be the same as 180° minus the ϕ coordinate of the corresponding electrode on the left, and ϕ coordinates of midline electrodes should be exactly 90° or 270°. By averaging θ and ϕ coordinates of left and right hemisphere electrodes and rounding to the nearest degree, we obtained the average angular (θ, ϕ) coordinates for each electrode shown in Fig. 4.

Although the angular coordinates of the measured electrodes differed from the expected ones (Fig. 3) by a relatively small amount in most cases, use of the average angular coordinates given in Fig. 4 may improve the accuracy of some analysis techniques, such as source dipole localization. Measurement of each subject's electrode locations at the time of recording (for example, using a commercial 3-dimensional digitizer) may further improve accuracy, especially when different technicians are involved in electrode placement.

References

Galambos, R., Perl, E.R. and Casby, J.U. Cortical localization of pure tone responses using a Laplacian electrode. Fed. Proc., 1953, 12: 48 (abst.).

Hjorth, B. An on-line transformation of EEG scalp potentials into orthogonal source derivations. Electroenceph. clin. Neurophysiol., 1975, 39: 526–530.

Law, S.K. and Nunez, P.L. Quantitative representation of the upper surface of the human head. Brain Topogr., 1991, 3: 365–371.

Nunez, P.L. Methods to estimate spatial properties of dynamic cortical source activity. In: G. Pfurtscheller and F.H. Lopes da Silva (Eds.), Functional Brain Imaging. Huber Publishers, Toronto, 1988: 3–9.

Pascual-Marqui, R.D., Gonzalez-Andino, S.L., Valdes-Sosa, P.A. and Biscay-Lirio, R. Current source density estimation and interpolation based on the spherical harmonic Fourier expansion. Int. J. Neurosci., 1988, 43: 237–249.

Perrin, F., Pernier, J., Bertrand, O., Giard, M.H. and Echallier, J.F. Mapping of scalp potentials by surface spline interpolation. Electroenceph. clin. Neurophysiol., 1987, 66: 75–81.

Perrin, F., Pernier, J., Bertrand, O. and Echallier, J.F. Spherical splines for scalp potential and current density mapping. Electroenceph. clin. Neurophysiol., 1989, 72: 184-187.

Salu, Y., Cohen, L.G., Rose, D., Sato, S., Kufta, C. and Hallett, M. An improved method for localizing electric brain dipoles. IEEE Trans. Biomed. Eng., 1990, 37: 699–705.

Wallin, G. and Stålberg, E. Source derivation in clinical routine EEG. Electroenceph. clin. Neurophysiol., 1980, 50: 282–292.